Project funded by the European Commission under the 6th (EC) RTD Framework Programme (2002- 2006) within the framework of the specific research and technological development programme “Integrating and strengthening the European Research Area”

Project UpWind

Contract No.:
019945 (SES6)

“Integrated Wind Turbine Design”

Single fibre and multifibre unit cell analysis of strength and cracking of unidirectional composites

AUTHOR:	Huaiwen WANG
AFFILIATION:	China University of Mining and Technology (Beijing)
ADDRESS:	Xueyuan Road D11, Beijing 100083, P. R. China
TEL.:	+86 10 62331286
EMAIL:	zhw@cumtb.edu.cn
FURTHER AUTHORS:	H. W. Zhou, L. Mishnaevsky Jr., P. Brøndsted, L. N. Wang
REVIEWER:	
APPROVER:	

Document Information

DOCUMENT TYPE	
DOCUMENT NAME:	Single fibre and multifibre unit cell analysis of strength and cracking of unidirectional composites
REVISION:	
REV.DATE:	
CLASSIFICATION:	R1: Restricted to project members
STATUS:	

Abstract: Numerical simulations of damage evolution in composites reinforced with single and multifibres are presented. Several types of unit cell models are considered: single fibre unit cell, multiple fibre unit cell with one and several damageable sections per fibres, unit cells with homogeneous and inhomogeneous interfaces, etc. Two numerical damage models, cohesive elements, and damageable layers are employed for the simulation of the damage evolution in single fibre and multi fibre unit cells. The two modelling approaches were compared and lead to the very close results. Competition among the different damageable parts in composites (matrix cracks, fibre/matrix interface damage and fibre fracture) was observed in the simulations. The strength of interface begins to influence the deformation behaviour of the cell only after the fibre is broken. In this case, the higher interface layer strength leads to the higher stiffness of the damaged material. The damage in the composites begins by fibre breakage, which causes the interface damage, followed by matrix cracking.

Contents

STATUS, CONFIDENTIALITY AND ACCESSIBILITY									
Status				**Confidentiality**				**Accessibility**	
S0	Approved/Released			**R0**	General public			Private web site	
S1	Reviewed			**R1**	Restricted to project members	**R1**		Public web site	
S2	Pending for review			**R2**	Restricted to European. Commission			Paper copy	
S3	Draft for commends			**R3**	Restricted to WP members + PL				
S4	Under preparation			**R4**	Restricted to Task members +WPL+PL				

PL: *Project leader* **WPL:** *Work package leader* **TL:** *Task leader*

1. Generation of Unit Cell Models of Composites with Damageable Elements

1.1 3D Unit Cells with Single and Multiple Fibres

A number of unit cell models of composites were generated with the use of the program code “Meso3DFibre”. The program generates a command file for the commercial FE pro- and post-processing software MSC/PATRAN©, which produces a 3D unit cell model of composite with pre-defined parameters. The 3D finite element meshes are generated by sweeping the corresponding 2D meshes on the surface of the microstructure models. The program “Meso3DFibre” is described in more details elsewhere.

Several unit cell models with single fibre and multi-fibres are shown in Fig. 1. The dimensions of the cell models are 10×10×10mm3. The unit cells were subject to a uniaxial tensile displacement loading along the axis of fibre (Z axis direction). The boundary conditions for all simulations were as follows: 1) for the bottom side of the cell model, all degree of freedoms of point (0, 0, 0) were fixed, the 3rd degree of freedom of bottom surface with coordinate z=0 was restricted, and the 1st degree of freedom of line with x=0 and z=0 was restricted; 2) for the other five sides of the cell model, the sides of the cube were fixed in such a way that all the nodes were bound together. So, each side could move only as a plane. Three-dimensional 6-node linear triangular prism element C3D6 was employed in this simulation for fibre, interface layer and matrix. The volume content of fibre is 4% in single-fibre model, which result in that the fibre diameter is 2.26mm.

The epoxy matrix composite reinforced with glass fibres was studied in this paper. Table 1 shows the properties of the phases used in the simulations. The data were taken from.

After the model was created in PATRAN©, the input file for FE commercial code ABAQUS© was generated. The simulations were carried out with ABAQUS©/STANDARD.

Table 1 Properties of the phases used in the simulations

	Young's modulus, GPa	Poisson's ratio	Failure criterion, MPa
Fibre	72	0.26	Single-fibre modelling: Constant fibre strength with different value in different model. Multi-fibre modelling: Weibull distribution with parameters σ0=929.8MPa and m=2.55.
Matrix	3.79	0.37	67 MPa
Interface	37.9	0.37	Different value in different model.

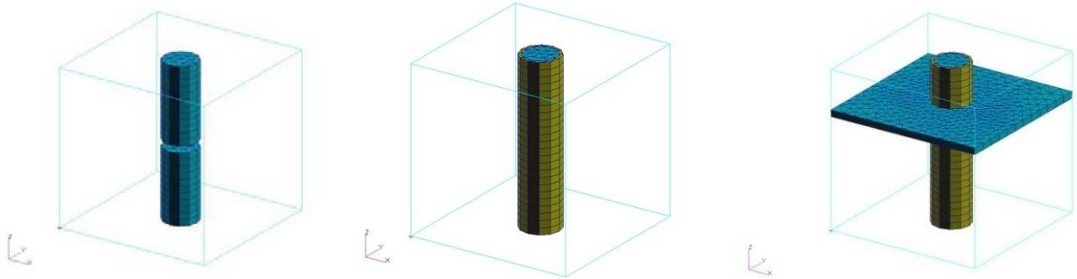

(a) (b) (c)

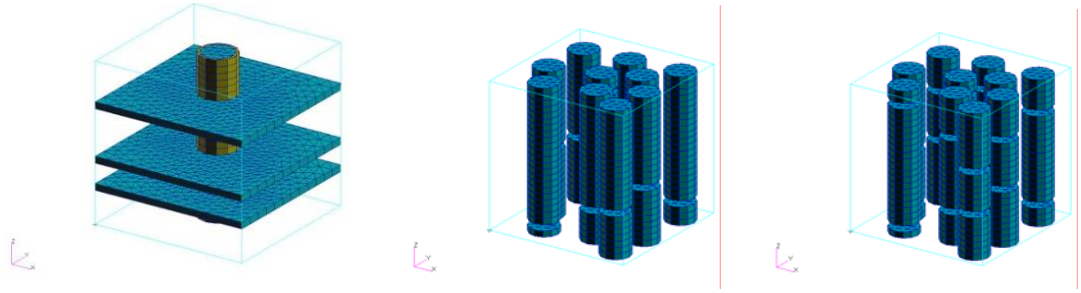

(d) (e) (f)

Fig 1. *FE microstructural models used in this study.*
(a) single-fibre model with one damageable layer in fibre, (b) single-fibre model with one damageable layer in fibre and fibre/matrix interface layer, (c) single-fibre model with one damageable layer in fibre, fibre/matrix interface and a damageable layer in the matrix, (d) single-fibre model with one damageable layer in fibre, one fibre/matrix interface and three damageable layers in the matrix, (e) multi-fibre model with one damageable layer per fibre, (f) multi-fibre model with two damageable layers per fibre

1.2 Techniques of modelling damage: damageable layer with element weakening techniques versus cohesive elements

In order to model breaking of fibres, two modelling techniques were employed: an approach based on the introducing damageable layer and the element weakening techniques, and the cohesive element model.

1.2.1 Damageable layer with element weakening techniques

The damageable layers were introduced into sections of fibres, following the idea by Gonzalez and LLorca. The damageable layers have the same mechanical properties as the rest of the fibre. The damage evolution in the damageable layers was modelled by using the finite element weakening method. In the framework of this method, the stiffness of a finite element is reduced if a stress parameter, such as maximum principal stress, in the element or a nodal point exceeds some critical level. This conditions was realised in the ABAQUS© subroutines User Defined Field. The subroutine checks whether the element failed or not according to the properties of the damageable layer.

A similar concept was used to simulate the matrix cracking and interface damage of composites. Following the idea from, we modelled the interface damage as a weakening of finite elements in a special “interface layer”. The interface was presented therefore as a special thin layer with thickness 0.2mm between the fibre and matrix. The damage evolution in this layer was modelled using the subroutine USDFLD as well.

1.2.2 Cohesive elements modelling

Most of the fibre reinforced composites materials exhibit elastic-brittle behaviour. There is less significant plastic deformation before damage initiation. A typical stress-strain relation is mostly linear-elastic in a first part and then tracked by degradation until the material fully losses its stiffness, which is called traction-separation response. There are three typical models to describe the post-damage process of a traction-separation, including exponential model, trapezoidal model and bilinear model. In this study, bilinear model was employed.

Damage initiation refers to the beginnings of the degradation of the response of a material point. The process of degradations begins when the stresses and/or strains satisfy certain damage criterion. Here maximum nominal stress criterion was selected, which was assumed to initiate when the maximum nominal stress ration reaches a critical value.

Once the damage initiation criterion is reached, the damage evolution describes the rate of degradation of the material. A scalar damage variable D is introduced to represent the overall damage process. D monotonically evolves from 0 (no damaged has occurred) to 1(overall damaged) upon further loading after damage initiation. The stress tensor is shown in Eqn. 1, where $\bar{t}$ represents the stress tensor if on damage occurs and t is the reduced actual stress tensor.

$$t = (1-D)\bar{t} \tag{1}$$

In the cohesive elements model, cohesive elements were placed in the damageable layers of fibres, matrix or interfaces. Three-dimensional 6-node linear triangular prism cohesive elements COH3D6 or three-dimensional 8-node linear brick cohesive elements COH3D8 were used in the cohesive layers. The cohesive elements connected to other elements by sharing nodes.

The stiffness of the cohesive elements was calculated as Young's modulus divided by the thickness of cohesive element, and was 172 GPa. The maximum nominal stress traction-interaction failure criterion was selected for the damage initiation in the cohesive elements, and the energy based damage evolution law is selected for damage propagation.

1.3 Determination of the damage criteria of the cohesive elements

Further, the simulations of the damage evolution in the microstructures with different cohesive elements damage initiation stress have been carried out, using the single fibre unit cell, shown in Fig. 1(a). Several levels of the damage initiation stress of cohesive elements have been taken: 100, 200, 300, 400, 500, 600, 700, 800, 900, 1000, 1100, 1200, 1250 and 1324MPa (the last value corresponds to the broken stress with damageable layer modelling). The plot of damage dissipation energy ALLDMD per unit area versus damage initiation stress is shown in Fig. 2.

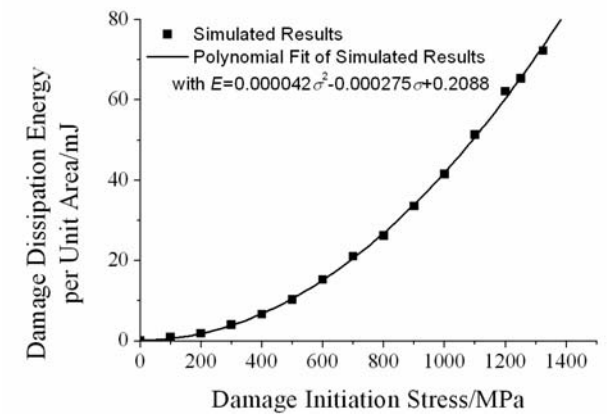

Fig. 2 *Damage dissipation energy per unit area versus damage initiation stress curve.*

Fig. 2 shows that the relation between the damage dissipation energy and the strength of the cohesive layer is nonlinear. The simulated results were fitted with a quadratic polynomial function using the least square method. The relation between damage dissipation energy per unit area and damage initiation stress can be expressed by

$$E = 0.000042\sigma^2 - 0.000275\sigma + 0.2088 \tag{2}$$

2. Computational experiments: Single-fibre unit cell models

In this section, the damage evolution in 3D single-fibre unit cell models is investigated. In so doing, the damageable layer with element weakening approach and cohesive elements modelling are used and compared.

2.1 Single fibre unit cell without damageable interface

In this section, single fibre unit cell models were employed to simulate damage evolution in composites. In the models, damage can occur only in the fibre.

2.1.1 Damageable layer versus cohesive element model

A single-fibre FE unit cell model with one damageable layer in fibre was considered here (see Fig. 1(a)). The damage evolution was modelled using two approaches: the weakening element layer model and the cohesive elements. Stress-strain and strain energy-strain curves as well as stress and strain distributions in the models were determined. Figures 3 and 4 show nominal stress-strain curves and strain energy-strain curve of the unit cell model, respectively. The maximal principal stress distributions before and after the fibre failure are shown in Fig. 5 and Fig. 6.

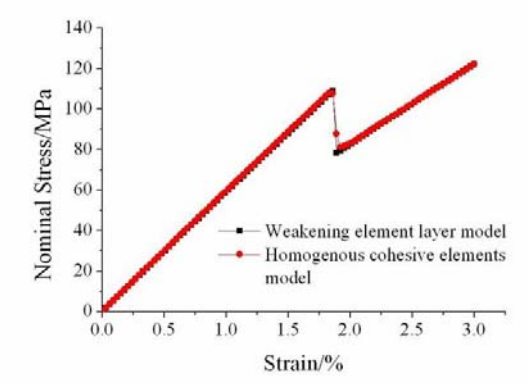

Fig. 3 *Nominal stress-strain curve of the cell models with different failure models.*

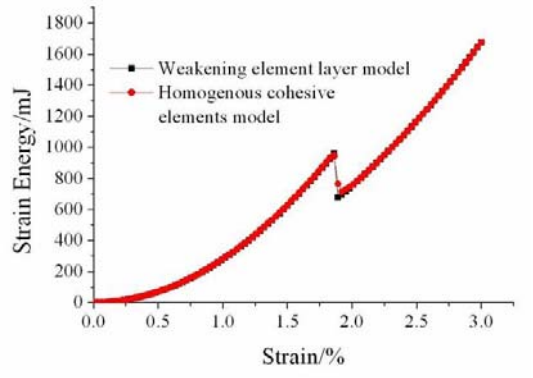

Fig. 4 *Strain energy-strain curve of the cell models with different failure models.*

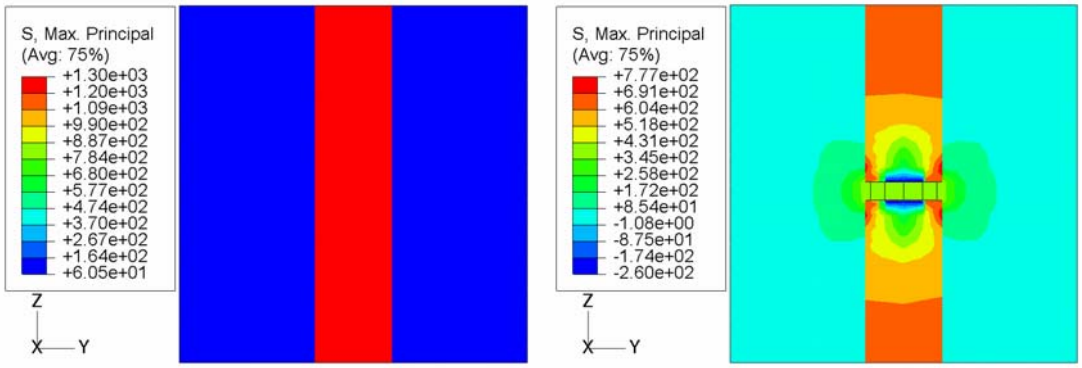

(a) Before damage initiation (ε=1.86%) *(b) Just after fibre is broken (ε=2.07%)*

Fig. 5 *Maximal principal stress distribution in damage evolution process (Damageable layer model).*

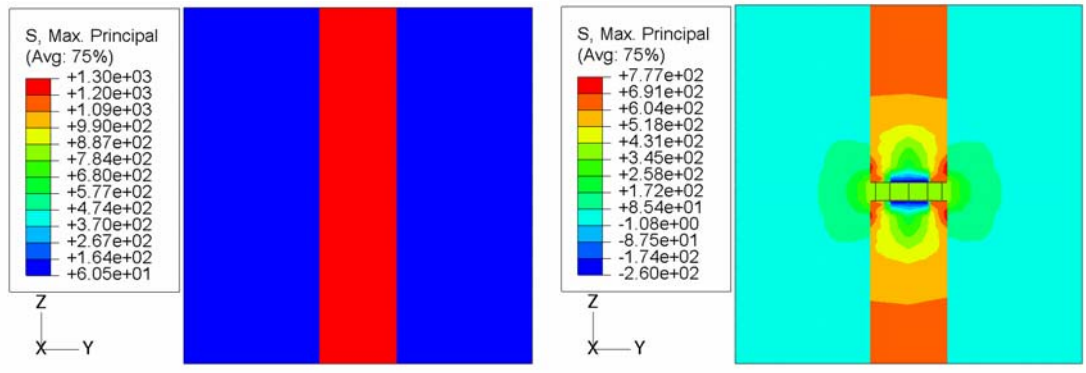

(a) Before damage initiation (ε=1.86%) *(b) Just after fibre is broken (ε=2.07%)*

Fig. 6 *Maximal principal stress distribution in damage evolution process (Cohesive elements model).*

From Fig. 3, one can see that the stiffness of the composite decrease at ε=1.86% for both models. However, in the case of damageable layer model, the maximum principal stress in the glass fibre decreases suddenly from 1.32×103MPa to 7.27×102MPa, as shown in Fig. 5. In the case of the cohesive elements model, the maximum principal stress in glass fibre decreased gradually from 1.30×103MPa to 7.77×102MPa (see Fig. 6). Simultaneously, the strain energy of the models decreases, as shown in Fig. 4.

From Figures 3-6, one can see that both models give very similar results regarding the overall response, failure point and the stress distribution. However, the stress evolution due to the fibre failure is different for the two considered damage models: the stress decrease suddenly in the case of the damageable layer model, and gradually in the case of the cohesive elements model.

2.1.2 Effect of local inhomogeneity of the damageable fibre material

In order to take into account the local, nanoscale heterogeneity of fibre material, we introduce the variability of element properties in the cohesive layer. An element at the edge of the cohesive elements layer was assigned a lower damage initiation strength (here, 600MPa was employed while other elements with 1200MPa).

The evolution processes of the damage variable SDEG (scalar stiffness degradation at integration points) for homogeneous cohesive layer model and inhomogeneous cohesive elements layer model are shown in Fig. 7 and Fig. 8. The nominal stress vs. strain curves and strain energy vs. strain curves are shown in Fig. 9 and Fig 10.

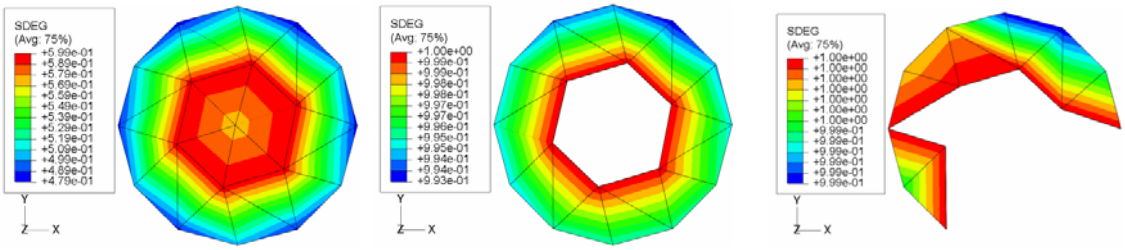

(a) ε=1.71% *(b) ε=1.83%* *(c) ε=1.89%*

Fig. 7 *Evolution of damage variable SDEG for homogeneous cohesive elements model*

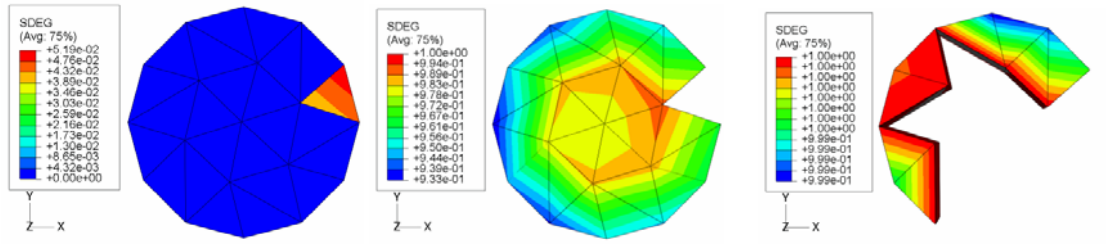

(a) ε=0.87% *(b) ε=1.71%* *(c) ε=1.89%*

Fig. 8 *Evolution of damage variable SDEG for inhomogeneous cohesive elements model.*

As expected, the damage initiation occurs at the weakest element and earlier for the case of the inhomogeneous cohesive elements model, than for the case of the homogeneous cohesive elements model (Fig. 7-8). However, the fibre breaks at the same strain of 1.92% in both models. From Fig. 9 and Fig.10, one can see that the stress-strain curves and strain energy-strain curves are very similar. However, it is notable that the damage begins at the centre, near the axis of the fibre in the case of the ideally homogeneous fibre strength properties. In the case of inhomogeneous fibre strength properties, the cracking in the fibre starts near the edge. Thus, while neglecting the local heterogeneity of fibre properties does not lead to large errors in estimating the global behaviour of composites, it does lead to a wrong picture of the damage evolution in the multiphase material.

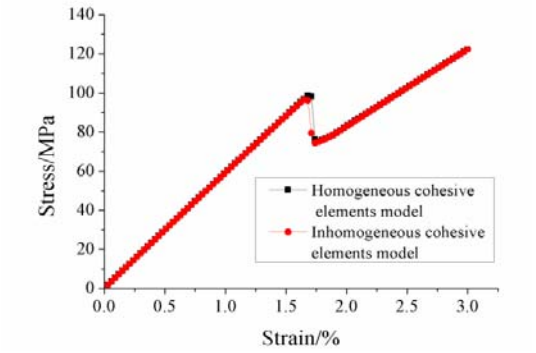

Fig. 9 *Nominal stress-strain curve of the cell models with different modelling.*

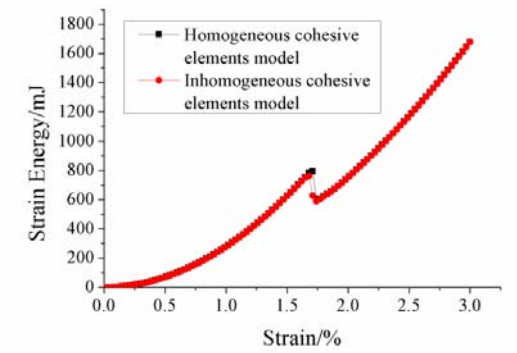

Fig. 10 *Strain energy-strain curve of the cell models with different modelling.*

2.2 Single fibre unit cell with damageable interface

In this section, damage evolutions in single fibre unit cell with damageable interface were carried out by different modelling techniques.

2.2.1 Comparison of two damage modelling techniques

A single-fibre FE microstructural model with interface (interphase) layer is shown in Fig. 1(b). In the framework of the damageable layer model, the interface was taken as a layer with finite thickness, made from a third material, with averaged materials properties of the fibre and matrix. The Young's modulus of interface material was assumed to 37.9GPa (the average value of the Young's modulus of fibre and that of the matrix) and Poisson's ratio 0.37 (the Poisson's ratio of the matrix). The interfacial shear strength between the fibre and the matrix is around 27 MPa. In this section, the values of fibre strength 1000 MPa and interfacial shear strength 30MPa are used.

Further, a single fibre unit cell model with damageable interface was generated using the cohesive elements. The three-dimensional 8-node linear brick cohesive elements COH3D8 were introduced in the interface layer. Similar to the cohesive elements in fibres, the stiffness of the cohesive elements at the interface was calculated as Young's modulus divided by the

thickness of cohesive element, and was 180 GPa. The maximum nominal stress traction-interaction failure criterion was selected for the damage initiation in the cohesive elements, and the energy-based damage evolution law is selected for damage propagation. The damage initiation stress was 30MPa. The fracture energy of the interface was calculated with the use of Eq. (2).

The stress-strain curves of the two cell models are shown in Fig. 11. One can see that the fibre breakage is observed in the cohesive model at slightly higher load, than in the damageable layer model. The reason is that while the elements in the damageable layer lose their stiffness stepwise, the stiffness lost by the cohesive elements is a monotonous function of strain.

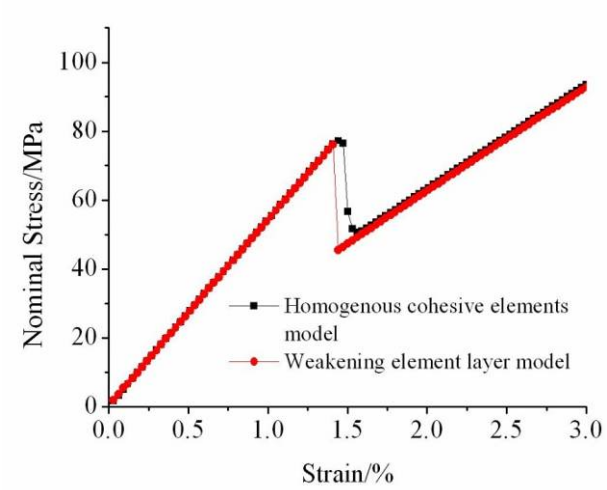

Fig.11 *Nominal stress-strain curve for a unit cell model of single fibre with interface layer.*

In order to see the process of damage evolution, the evolution of damage variable SDEG in the two damageable parts is shown in Fig. 12. It can be seen that the fibre cracking begins earlier than the interface damage, though the strength of fibre (1000MPa) is much higher than that of interface (30MPa). After the fibre is broken, the damage at the interface is growing rapidly.

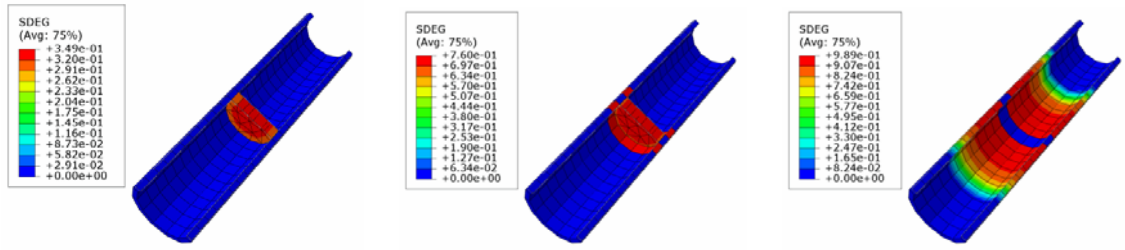

(a) ε= 1.44% *(b) ε=1.47%* *(c) ε= 1.50%*

Fig. 12 *Evolution of damage variable SDEG for all cohesive elements.*

2.2.2 Effect of interface and fibre strengths on the effective response of the composite cell

In order to study the competition between the two damage parts in composites (interface damage and fibre fracture), two series of simulations were carried out.

In the first series of simulations, the strength of interface layer was varied, while the strength of fibre was assumed to be constant. Several levels of the critical stress of interface layer have been taken: 100, 200, 300 and 400MPa. The strength of the fibre was 900MPa. The nominal stress-strain curves of the cells model in this case are shown in Fig. 13.

In the second series of simulations, the strength of fibres was varied, while the strength of interface layer was kept constant. Several levels of the critical stress of fibre have been taken: 600, 700, 800, 900 and 1000 MPa. The interface strength was 300MPa. The nominal stress-

strain curves of the cell models in this case are shown in Fig. 14.

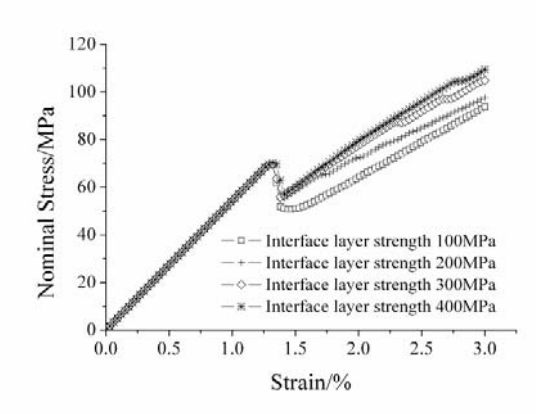

Fig. 13 *Nominal stress-strain curve for unit cell models of single fibre with interface layer with different interface strength.*

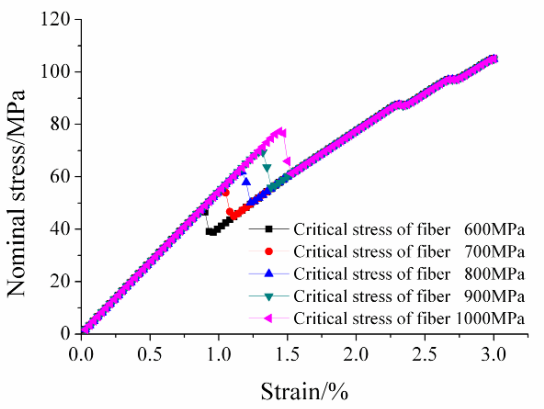

Fig. 14 *Nominal stress-strain curve for unit cell models of single fibre with interface layer with different fibre critical strength.*

From Figure 13 it can be seen that the interface layer strength has no effect on the effective response of the composite with intact fibres. However, after the fibre is broken, the higher the stiffness of the composite, the higher is the interface layer strength.

Figure 14 also shows that the strength of the fibre has more effect on the pre-critical load of the cell model. The higher fibre critical stress, the later is it broken. So it is an effective approach to improve the load capacity by employing high strength glass fibre.

2.2.3 Inhomogeneous cohesive elements in the interface layer

Let us consider the effect of the inhomogeneity and variability of the local interface properties on the strength of composite. In order to study the effect of the variability of local interface properties, we introduced various cohesive elements in the interface layer of the single fibre unit cell. 288 cohesive elements (with correspondingly 288 various material properties, with random strengths) were placed in the interface layer. The strengths of interface elements were varied randomly from 100MPa to 200MPa, according to the uniform probability distribution law.

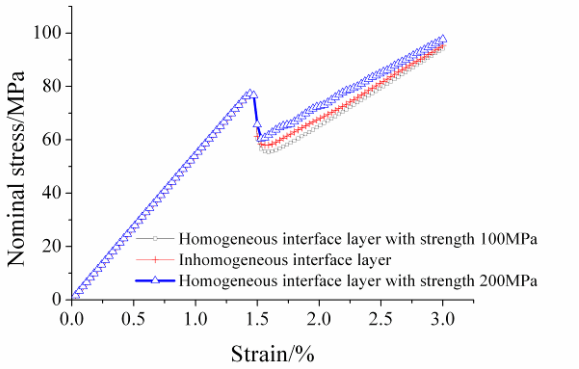

Fig. 15 *Stress-strain curves for homogeneous and inhomogeneous interface layers.*

One can see from Figure 15 that the effective response of the model with the interface layer with random varied local properties is just between the corresponding curves for the cases of constant strengths of interfaces. One can conclude that the variability of local interface properties does not have any major effect on the composite strength, apart from the effect of the averaged interface strength. Thus, it is enough to take into account the averaged interface strength, and not its variability, in the damage simulations of composites. However, this

conclusion was tested only for tensile loading along the fibre axes; most probably, it can be generalized for shear or compressive loading of composites.

2.3 Competition among different damage modes in composites

In this section, we seek to consider the interaction among all three damage modes in composites (matrix cracks, fibre/matrix interface damage and fibre fracture), and the sequence of damageable evolution.

2.3.1 Single fibre model with one matrix crack and homogeneous interface layer

A single-fibre FE cell model with cracked fibre, damaged matrix/fibre interface and one matrix crack is shown in Fig. 1(c). Additionally to the single fibre model with damageable interface considered above, this model allows the damage and cracking on matrix. Three-dimensional 6-node linear triangular prism cohesive element COH3D6 was employed in the damageable layers in the fibre and matrix. Three-dimensional 8-node linear brick cohesive element COH3D8 was employed in fibre/matrix interface layer. Correspondingly, three cohesive materials with the following strengths were created: 600, 100 and 67 MPa (fibre fracture, interface and matrix crack, respectively). The displacement load along the fibre axis is 0.135mm. The evolution of damage variable SDEG in the three damageable parts is shown in Fig. 16. The nominal stress-strain curve of the cell model is shown in Fig. 17.

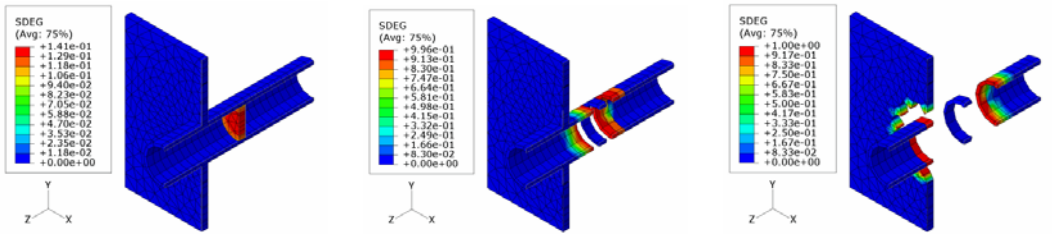

(a) ε=0.85% *(b) ε=1.10%* *(c) ε=1.35%*

Fig. 16 *Evolution of damage variable SDEG of the model*

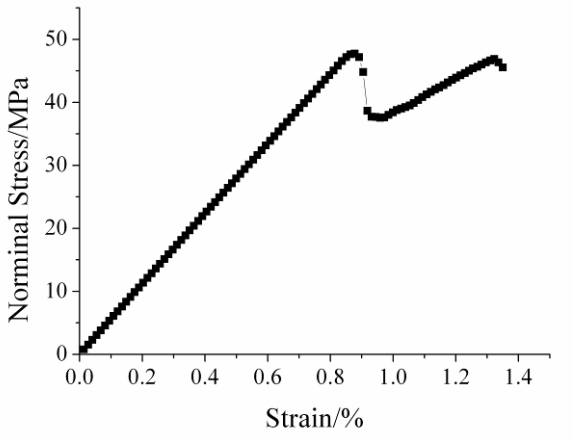

Fig. 17 *Nominal stress-strain curve for unit cell models of single fibre with interface layer and matrix crack.*

From Fig. 16, one can see that the sequence of damage evolution in this case is as follows: first, fibre cracking, then interface debonding, and, finally, the matrix crack damages at last. The stiffness of composites is drastically reduced after the fibre failure. The composite with the failed

fibre deforms elastically, with the reduced Young's modulus. Further reduction of the composite stiffness takes place when the matrix cracking begins.

2.3.2 Multiple matrix cracking

In this section, we consider the multiple cracking in the matrix and its interaction with interface debonding and fibre cracking. A single fibre unit cell model with three damageable layers in matrix (additionally to the damageable layers in the interface and fibre) is shown in Fig. 1(d).

The material properties were the same as in the previous model. The interface strengths were taken at two levels: 100MPa and 200MPa. Further, for the case of inhomogeneous interface, the randomly distributed strengths between 100MPa to 200MPa were assigned to the elements on the interface.

In the simulations, it was observed that the matrix crack, which is closest to the fibre fracture, begins to grow first, and the other two potentially damageable layers do not get damaged. The nominal stress-strain curves for different interface strengths are shown in Fig. 18.

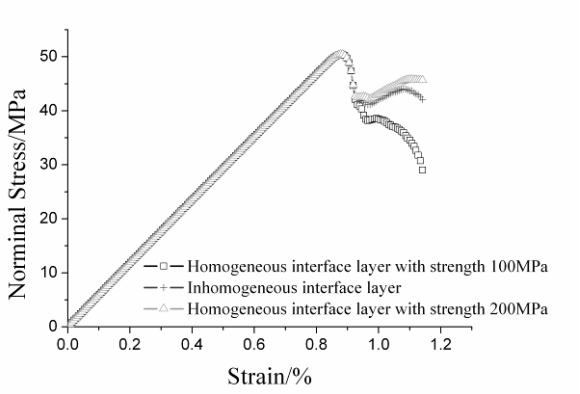

Fig. 18 *Nominal stress-strain curves for unit cell models of single fibre with interface layer and three matrix cracks with two different interface strength.*

It can be seen from Fig. 18 that the matrix cracking strongly depends on the interfacial strength of composite: the higher the interfacial strength, the less matrix damage. Depending on the interface strength, the composite can keep rather high stiffness after the fibre failure (the case of the interface layer strength 200 MPa), or its stiffness will continue to fall (the interface layer strength 100 MPa). Thus, the high interfacial strength may compensate for the brittleness of matrix, and delay the matrix cracking in the composites.

Comparing Figures 15 and 18, one can state that the interface strength has a very weak influence on the composite behaviour in the case of strong, non-damageable matrix, and a very strong influence on the composite stiffness in the case of weaker, brittle matrix.

3. Single-fibre versus multi-fibre modelling: Effect of fibre crack interaction

In this section, we consider the effect of multiple fibres, interaction between many fibre cracks and other defects on the strength and damage evolution in composites.

3.1 Multifibre unit cell model: Cohesive elements versus damageable layer model

Let us consider the effect of multiple fibres on the damage evolution in the composite. 10-fibre unit cell model, generated by the program code “Meso3DFibre” is shown in Fig.1 (e). Every fibre in the cell has one damageable layer, randomly placed along the fibre axis. The volume content of fibres was taken 34%. The fibre strength distribution follows Weibull probability law with parameters $\sigma 0$=929.8MPa and m=2.55. The boundary conditions were described in section 3. Two modelling methods, damageable layer model and cohesive elements modelling, were

employed to study the damage evolution.

The nominal stress-strain curves of the cell model are shown in Fig. 19. In this model, only fibres are considered to be damageable. The matrix and interface are supposed to be very strong and non-damageable.

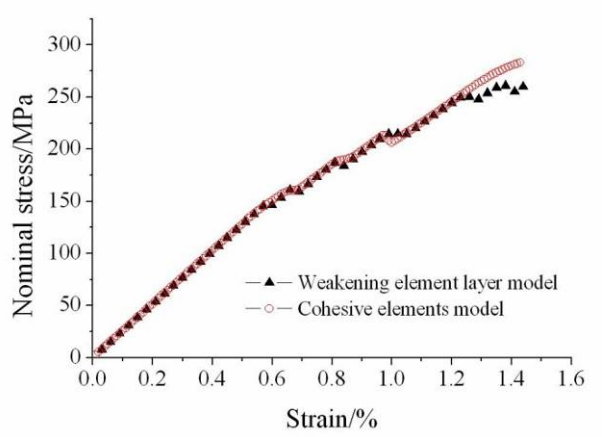

Fig. 19 *Nominal stress-strain curves for unit cell models of multifibre with one damageable layer.*

Comparing Figures 3 and 19, one can see that the model is more sensitive to the method used in the case of multifibre cell, than in the case of single the fibre unit cell. As expected, the stress-strain curve in the case of multifibre model has a zigzagged shape.

3.2 Effect of multiple fibre cracking

In this subsection, we seek to study the effect of possibility of multiple cracking in each fibre on the strength and damage evolution in composites. We used 10-fibre unit cell model, similar to that shown in Fig. 1(f). However, two (not one) damageable layers were placed in every fibre. The locations of both damageable sections were determined using the random number generator. From totally 20 damageable layers in 10 fibres, each damageable layer was assigned its own strength, following the Weibull probability law with parameters $\sigma 0$=929.8MPa and m=2.55.

The nominal stress-strain curves of the multifibre unit cell models with one and two damageable layers are shown in Fig. 20.

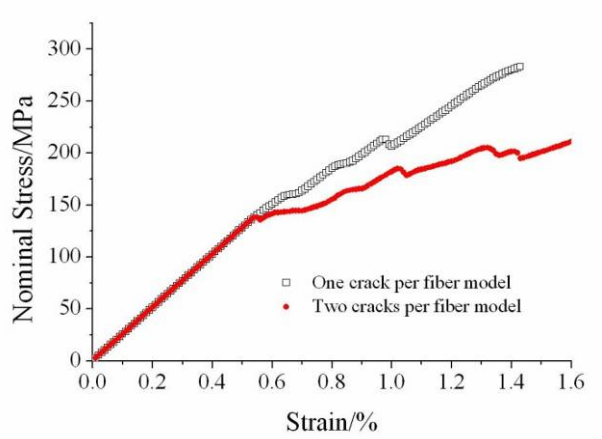

Fig. 20 *Nominal stress-strain curves of the multifibre unit cell models with one and two damageable layers per fibre.*

One can see from Fig. 20 that the possibility of multiple cracking of fibres does influence the stiffness and damage growth in composites (in contrast to the possibility of multiple cracking in matrix!). The loss of stiffness due to the multiple fibre cracking is much bigger than that due to the single fibre cracking.

Figures 21 shows the stress-strain curves together with the damage strain curves. The damage is calculated as an amount of failed finite elements in fibres. One can see that the zigzags on the stress-strain curve correspond to the fibre cracking events.

Figure 22 shows the Mises stress distribution before and after the second cracking in a fibre. The stresses are highest in the matrix regions between two neighbouring fibre cracks. One can see from the Figures 22a and 22b, that the second cracking in an already cracked fibre takes place rather closely to, and in the area of high stress concentration of a crack in another, adjacent fibre. Thus, the cracks in the fibres can induce the cracking in neighbouring fibres.

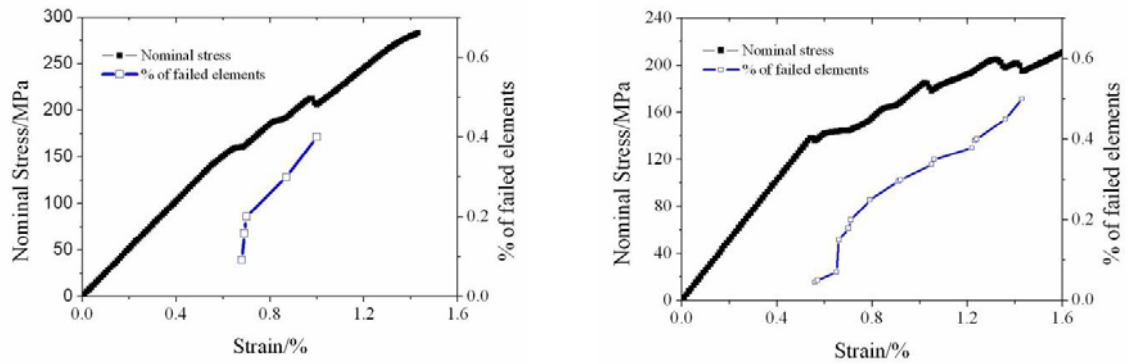

(a) One crack per fibre model *(b) Two cracks per fibre model*

Fig. 21 *Nominal stress and % of failed elements versus strain curves for multifibre models with one and two cracks per fibre.*

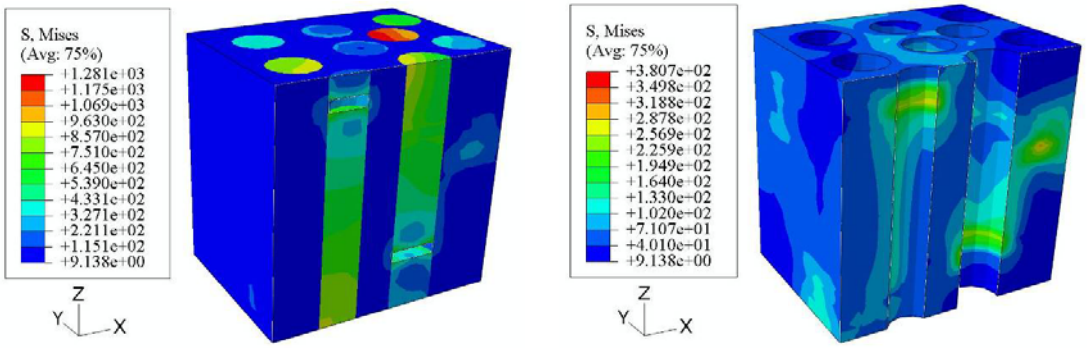

(a) Before the second crack in a fibre ε=1.41% (with and remove fibres)

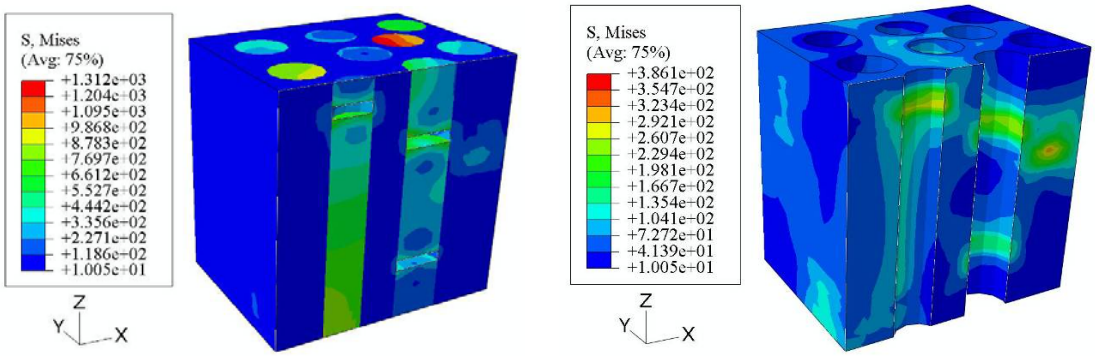

(b) (b) After the second crack in the fibre ε=1.43% (with and remove fibres)

Fig.22 *Mises stress distribution before and after the second crack in one fibre full damaged.*

4. Conclusion

In this study, the simulations of damage evolution in fibre reinforced composites, based on different modelling techniques and seeking to clarify the effects of interface strength, interface homogeneity, interaction between cracks in different phases on the strength and damage evolution in the composites.

The computational investigations lead us to the following conclusions:

(1) In the considered material, the sequence of damage evolution can be described as follows: first, fibre cracking, then interface debonding, and, finally, the matrix crack damages at last. The fibre cracking begins earlier than the interface damage, though the strength of fibre is much higher than that of interface. After the fibre is broken, the damage at the interface is growing rapidly. The stiffness of composites is drastically reduced after the fibre failure. The composite with the failed fibre deforms elastically, with the reduced Young's modulus. Further reduction of the composite stiffness takes place when the matrix cracking begins.

(2) The strength of the interface layer has no effect on the effective response of the composite under tensile loading before the fibres begin to crack. However, after the fibre is broken, the stiffness of the composite is the higher, the higher interface layer strength.

(3) The variability of local interface properties does not have any special effect on the tensile strength of composites, apart from the effect of the averaged interface strength. It is therefore enough to take into account the averaged interface strength, and not its variability, in the damage simulations of composites.

(4) The matrix cracking strongly depends on the interfacial strength of composite: the higher the interfacial strength, the less matrix damage. Depending on the interface strength, the composite can keep rather high stiffness after the fibre failure, or its stiffness will continue to fall. Thus, the high interfacial strength may compensate for the brittleness of matrix, and delay the matrix cracking in the composites. The interface strength has a very weak influence on the composite behaviour in the case of strong, non-damageable matrix, and a very strong influence on the composite stiffness in the case of weaker, brittle matrix.

(5) It was observed in the simulations that the second cracking in an already cracked fibre takes place rather closely to, and in the area of high stress concentration of a crack in another, adjacent fibre. Thus, the cracks in the fibres can induce the cracking in neighbouring fibres.

As differed from single fibre unit cells, the multifibre cells allows to take into account the interaction between competing damage mechanisms, multiple fibre breaks, etc. The study of damage evolution in multi-fibre models is to be continued in the forthcoming works.

References

[1] L. Mishnaevsky Jr., Computational Mesomechanics of Composites, John Wiley and Sons, London, 2007.

[2] L. Mishnaevsky Jr., P. Brøndsted, Micromechanisms of damage in unidirectional fiber reinforced composites with polymer matrix: 3D computational analysis, Composites Science and Technology, Accepted. DOI: 10.1016/j.compscitech.2009.01.022

[3] L. Mishnaevsky Jr., P. Brøndsted, Mater. Sci. Eng. A, 498(2008)81-86

[4] A.M. Sastry, S.L. Phoenix, J. Mater. Sci. Lett., 12(1993)1596.

[5] C.M.Landis, I.J. Beyerlein, R. M. McMeeking, J. Mech. Phys. Solids, 48(2000)621.

[6] I.J.Beyerlein, S.L. Phoenix, J. Mech. Phys. Solids, 44(1996)1997.

[7] Z. Xia, W. A. Curtin, T. Okabe, Compos. Sci. Technol., 62(2002)1279.

[8] F. Kun, S. Zapperi, H.J. Herrmann, Eur. Phys. J. B, 17(2000)269.

[9] F.Raischel, F. Kun, H.J. Herrmann, Phys. Rev. E, 73(2006) 66101.

[10] D.B. Marshall, B.N. Cox, A.G. Evans, Acta Metall., 33(1985)2013.

[11] L.N. McCartney, Proc. R. Soc. Lond. A, Math. Phys. Sci., 409(1987)329.

[12] W.S. Slaughter, Int. J. Solids Struct., 30(1993)385.

[13] L. Mishnaevsky Jr., S. Schmauder, Appl. Mech. Rev., 54(2001)49.

[14] D. Ouinas, B. Serier, B.B. Bouiadjra, Comput. Mater. Sci., 39(2007)782.
[15] M.R. Kabir, W. Lutz, K. Zhu, S. Schmauder, Comput. Mater. Sci.,36(2006)361.
[16] G.I. Giannopoulos, D. Karagiannis, N.K. Anifantis, Comput. Mater. Sci., 39(2007)437.
[17] T. Rahman, W. Lutz, R. Finn, S. Schmauder, S. Aicher, Comput. Mater. Sci., 39(2007)65.
[18] K. Zhu, S. Schmauder, Comput. Mater. Sci., 28(2003)743.
[19] S. Feih, A. Thraner, H. Lilholt, J. Mater. Sci., 40(2005)1615.
[20] G. Debotton, L. Tevet-Deree, J. Compos. Mater., 38(2004)1255.
[21] J. M. L. dos Reis, Mater. Res., 8(2005)357.
[22] Gudapati KBV Kumar, Studying the influence of glass fiber sizing roughness and thickness with the single fiber fragmentation test. Kristianstad University, Degree Project, 2006.
[23] C. Gonzalez, J. LLorca, Acta Mater., 54(2006)4171.
[24] L. Mishnaevsky Jr., Compos. Sci. Technol., 66 (2006)1873.
[25] L. Mishnaevsky Jr., Mater. Sci. Eng. A, 407(2005)11.
[26] ABAQUS 6.7. User's Manual, Abaqus Inc. Providence, RI, USA, 2007
[27] Anna Brugger. Diploma thesis, Universität Karlsruhe (TH), 2006